Brachial Plexus Anatomy of Miniature Swine Compared to Human

Amgad S Hanna (ah2904@yahoo.com)
Deparment of Neurological Surgery, University of Wisconsin Madison https://orcid.org/0000-0002-5062-5952

Daniel Hellenbrand
Department of Neurological surgery, University of Wisconsin School of Medicine and Public Health (UWSMPH) – Madison

Dominic Schomberg
Department of Animal and Dairy Sciences, University of Wisconsin – Madison

Shahriar M Salamat
Departments of pathology and laboratory medicine, and Neurological Surgery, University of Wisconsin School of Medicine and Public Health (UWSMPH) – Madison

Megan Loh
Department of Neurological surgery, University of Wisconsin School of Medicine and Public Health (UWSMPH) – Madison

Lea Wheeler
Department of Neurological surgery, University of Wisconsin School of Medicine and Public Health (UWSMPH) – Madison

Barbara Hanna
University of Wisconsin – Madison

Burak Ozaydin
Department of Neurological surgery, University of Wisconsin School of Medicine and Public Health (UWSMPH) – Madison

Dhanansayan Shanmuganayagam
Department of Animal and Dairy Sciences, University of Wisconsin – Madison Department of Surgery, University of Wisconsin School of Medicine and Public Health (UWSMPH) – Madison

---

Research

Keywords: anatomy, avulsion, brachial plexus, nerve injury, swine

Posted Date: August 19th, 2020

DOI: https://doi.org/10.21203/rs.3.rs-54092/v1

Version of Record: A version of this preprint was published at Journal of Anatomy on August 6th, 2021.
See the published version at https://doi.org/10.1111/joa.13525.

Abstract

Background: Brachial plexus injury (BPI) occurs when the brachial plexus is compressed, stretched, or avulsed. Although rodents are commonly used to study BPI, these models poorly mimic human BPI due to the discrepancy in size. The objective of this study was to compare the brachial plexus between human and Wisconsin Miniature Swine™ (WMS™), which are approximately the weight of an average human (68–91 kg), to determine if swine would be a suitable model for studying BPI mechanisms and treatments.

Methods: To analyze the gross anatomy, WMS brachial plexi were dissected both anteriorly and posteriorly. For histological analysis, sections from various nerves of human and WMS brachial plexi were fixed in 2.5% glutaraldehyde and then myelinated axons were labeled using 2% osmium tetroxide before being counter-stained with Masson's Trichrome.

Results: Gross anatomy revealed that the separation into 3 trunks and 3 cords is significantly less developed in the swine than in human. In swine, it takes the form of upper, middle, and lower systems with ventral and dorsal components. Histological results showed that despite the similarity in body size between the miniature swine model and humans, there was some discrepancy in nerve size and the number of the myelinated axons. The WMS had significantly fewer myelinated axons than humans in median ($p = 0.0009$), ulnar ($p = 0.0001$), and musculocutaneous nerves ($p = 0.0451$). The higher number of myelinated axons in these nerves for humans is expected, because there is a high demand of fine motor function in the human hand, with more motor units. Due to the stronger shoulder girdle muscles in WMS, the WMS suprascapular nerves were larger than in human.

Conclusion: Overall, the WMS brachial plexus is similar in size and origin to human making them an excellent model to study BPI. Future studies analyzing the effects of BPI in WMS should be conducted.

Background

The brachial plexus is a network of nerves formed by the ventral rami of the four lower cervical nerves (C5, C6, C7, C8) and the first thoracic nerve (T1), with some variability amongst different species. Brachial plexus injury (BPI) is a nerve injury defined by loss of function in one or both upper limbs resulting from partial or complete denervation of muscles. A BPI may occur when this network of nerves is compressed, stretched, or, in more serious cases, avulsed. Approximately 1.2% of multi-trauma patients suffer from some form of BPI, and the majority of these injuries are caused by high velocity traffic collisions [1]. Adult patients with BPI are, on average, young men between the ages of 25 and 29 and go on to suffer socioeconomic disadvantages, physical disabilities, and a decreased quality of life [2–4].

BPI can restrict upper limb function in a variety of ways. Injury to C5-C6 nerves causes loss of elbow flexion, shoulder abduction, and external rotation. Deficits in movements of the fingers and wrist indicate involvement of C7 and C8 spinal nerves [5]. Sensory and motor deficits are accompanied by neuropathic pain in up to 95% of BPIs and can be extremely debilitating [6, 7]. Secondary signaling cascades,

including inflammation, oxidative stress, blood-spinal cord barrier destruction, and scar formation, further exacerbate the injury and negatively impact recovery [8–11].

Treatment for BPI has been unsatisfactory due to the complexity of the injury and the lack of specific treatments [12]. Brachial plexus avulsion (BPA) is a preganglionic lesion and is the most severe form of BPI; it is extremely difficult to treat [13]. Current treatment methods of BPI include distal nerve transfers, brachial plexus exploration, nerve grafting from residual nerves, free muscle transfers, and tendon transfers [14]. Despite recent advances in nerve repair techniques, the prognosis of BPA, especially panplexus injuries, is generally poor [5, 14].

Highly translatable animal models are required to recapitulate the anatomy and complex pathophysiology associated with BPI. Rats and mice are the most-often studied animal model and represent a majority of scientific literature[15]. These models are low cost, have well-established analysis methods, and have easily manageable husbandry. However, these studies fail to produce satisfactory results in human clinical trials, likely due to differences in size, physiological responses, and anatomy [16]. A lack of comparative studies on descending neural pathways, differences in segmental injury distribution, and difficulty estimating international treatment standards also contribute to the failure of clinical trials [17, 18]. These limitations may be more easily overcome with a better intermediary animal model. Larger animals such as swine have shown to be a valuable translational resource for modeling more complex pathophysiology. Similarities in body size, physiological responses, and anatomical dimensions to humans make swine an excellent translational model [19]. Conventional breeds of pigs typically reach 100 kg by 4 months of age and 249–306 kg at full maturity and are impractical for use in long-term studies. In contrast, the Wisconsin Miniature Swine™ (WMS™) range from 25–50 kg at 4 months of age and 68–91 kg at full maturity, approximating the weight of an average human, and can be maintained at adult human size for years [18]. The low cost, short gestation interval, and high availability of swine are also advantages over the non-human primate models that are traditionally more costly. Swine share ten times the number of orthologous gene families with humans compared to rodent models and have an analogous inflammatory marker profile post-injury [20, 21]. Similarities between swine and humans in dietary structure, kidney function, respiratory rates, and social behaviors further advance their suitablility as a medical animal model [22]. Swine have more recently been used for translational research in cardiology, diabetes, traumatic brain injury, and spinal cord injury [23–26]. The purpose of this study is to perform an in-depth anatomical comparison of the brachial plexus between humans and WMS to determine suitability as a model for BPI treatment research.

Methods

Swine dissection

Four male WMS (weight = 76.8 kg ± 1.22 kg; age = 502 ± 1 days) bred and maintained at the Swine Research and Teaching Center (SRTC; University of Wisconsin-Madison) were euthanized and six brachial plexuses were dissected. Euthanasia started with sedation using TELAZOL® / xylazine, anesthesia with

isoflurane, then intracardiac administration of saturated potassium chloride solution. These were exposed both anteriorly and posteriorly. Anterior exposure was done through an axillary incision. After cutting the pectoral muscles, the forelimb was abducted for full exposure of the brachial plexus. Posterior exposure was performed through a cervicothoracic laminectomy and resection of the paraspinal muscles.

Histological analysis

Median, ulnar, musculocutaneous, and suprascapular nerves were harvested from three WMS. For comparison, median, ulnar, and musculocutaneous nerves were obtained from three fresh human cadavers, and a suprascapular nerve was taken from a formalin-fixed cadaver (Table 1). Since post-processing steps can cause the tissue to shrink[27], we made sure all fixation and processing steps were consistent for both WMS nerves and fresh human nerves. For fixation, all nerve segments were submerged in 0.1 M PBS, containing 2.5% glutaraldehyde, for a minimum of 24 hours. To view myelinated axons, 1 mm nerve segments were rinsed twice in 1X PBS, placed in 2% osmium tetroxide in 1X PBS for 2 hours, dehydrated in ethanol, and paraffin-embedded [28]. The paraffin-embedded segments were then sectioned transversely 5 μm thick and placed on glass slides. The sections were counter-stained with Masson's Trichrome (Sigma) and cover-slipped with Permount. Two slides from each nerve segment were not counterstained and left with only the osmium tetroxide fixation for counting myelinated axons.

All sections were imaged under the same parameters at 20X on a Keyence BZ-9000. An assessment of the myelinated axons was conducted using the Keyence BZ-II Analyzer software. The same threshold for all images was used, the axons were filled, and the total area of each myelinated axon was recorded. Only myelinated axons larger than 1 μm in diameter were analyzed. Nerve cross-sectional area was measured using ImageJ.

Statistics

Statistical analyses were performed using the unpaired, two-tailed Student's T-Test in Prism 6 (GraphPad Software, San Diego, CA). Differences were considered significant at $p < 0.05$. Quantitative data are presented as mean ± standard error of the mean (SEM).

Results

Gross anatomy

The WMS skeleton does not have a clavicle. The spinous processes of C3-C6 are short and C7 is longer, but T1 is considerably longer and is a very important landmark. One unique feature of the cervical vertebrae is the presence of a ventral branch of the transverse process that covers the most proximal part of the brachial plexus anteriorly. Distal to the dorsal root ganglion, the spinal nerves divide into ventral and dorsal rami that exit the spinal canal through separate foramina. The brachial plexus is formed by the ventral rami of C6-C8 with variable contribution from C5, T1, and occasionally T2. The separation into

3 trunks and 3 cords is significantly less developed in the WMS. There are upper, middle, and lower systems with ventral and dorsal components (Figs. 1 & 2). The upper system predominantly arises from C6 with some contribution from C5 and goes primarily to the suprascapular nerve. The middle system is mainly C7 and supplies the axillary nerve. The lower system is predominantly C8 with some contribution from T1 and is the main supply to the distal forelimb through the median and ulnar nerves as its ventral components, as well as the radial nerve as its dorsal component. An interesting finding is that the 3 systems are tightly interconnected with side branches, making it extremely difficult to decide on the exact spinal level contribution to each nerve. Numerous pectoral nerves arise proximally to supply the robust pectoral muscles. The suprascapular nerve has the largest diameter while the musculocutaneous nerve has the smallest. The latter has dual origin, typically from C7 and C8.

Histology

The median nerves were not significantly different in size between the WMS and human (WMS = 10.29 ± 0.94mm^2, Human = 9.99 ± 0.59mm^2, p = 0.7986). The WMS median nerves had significantly fewer myelinated axons than human median nerves (WMS = 19,625 ± 1561, Human = 34,798 ± 747, p = 0.0009), and the axons were not significantly different in size (WMS = 51.97 ± 0.47μm^2, Human = 43.66 ± 6.31μm^2, p = 0.2598) (Fig. 3).

The WMS ulnar nerves were significantly larger than human ulnar nerves (WMS = 7.24 ± 0.11mm^2, Human = 6.61 ± 0.13mm^2, p = 0.0190). Although the WMS ulnar nerves had significantly fewer myelinated axons than human ulnar nerves (WMS = 16,725 ± 521, Human = 24,633 ± 117, p = 0.0001), the axons in WMS ulnar nerves were significantly larger (WMS = 43.15 ± 1.45μm^2, Human = 34.04 ± 2.76μm^2, p = 0.0429) (Fig. 4).

The musculocutaneous nerves were not significantly different in size between the WMS and human (WMS = 2.66 ± 0.17mm^2, Human = 1.99 ± 0.39mm^2, p = 0.1958). The WMS musculocutaneous nerves had significantly fewer myelinated axons than human musculocutaneous nerves (WMS = 2237 ± 159, Human = 4936 ± 924, p = 0.0451), and the axons in WMS musculocutaneous nerves were also significantly larger (WMS = 69.17 ± 2.55μm^2, Human = 25.08 ± 0.75μm^2, p < 0.0001) (Fig. 5).

The suprascapular nerves appeared much larger in WMS than in humans (WMS = 13.77 ± 0.19mm^2, Human = 7.68mm^2). The WMS suprascapular nerves had more myelinated axons than human suprascapular nerves (WMS = 10,060 ± 1228, Human = 8270), and the axons in WMS suprascapular nerves were larger (WMS = 68.62 ± 5.72μm^2, Human = 24.65μm^2) (Fig. 6).

Discussion

The present study focuses on the WMS model and its applicability for researching BPI. Overall, this study demonstrates that the WMS brachial plexus closely resembles the human brachial plexus in comparison to other non-primate vertebrate models [29]. The similarities can be appreciated through previous

research with swine model post-avulsion injury retaining more similarities to human models in terms of motor neuron death compared to small animal models [30, 31]. The differences in physiological responses between these models may be due to species-specific responses or age differences [5]. The lack of clinically-relevant therapies in rodent models despite their widespread use has resulted in more studies shifting their focus towards larger animal models. Miniture swine are comparable to humans from an anatomical, physiological, and pathophysiological perspective, making them an ideal model for BPI studies [32].

In general, our anatomical results for the brachial plexus in WMS were consistent with previous findings in domestic pigs and wild boar [33, 34]. The WMS ulnar nerve resulted from the union of C7, C8, and T1 (Fig. 2). Although, the WMS ulnar nerve was slightly larger than human ulnar nerves, the WMS ulnar nerve had fewer myelinated axons that were, on average, larger than those in human ulnar nerves (Fig. 4). The WMS median nerve also resulted from the union of C7, C8, and T1 (Fig. 2). The WMS median nerve was similar in size to the human median nerve; the fascicles, however, appeared smaller with significantly fewer myelinated axons in the WMS median nerve (Fig. 3). The WMS musculocutanous nerve originated from C7 and C8 (Fig. 2). Similar to other nerves, the WMS musculocutanous nerve had fewer myelinated axons that were significantly larger than what was observed in the human musculocutanous nerves (Fig. 5). The more numerous myelinated axons in the human ulnar and median nerves are likely due to the demand of fine motor functions in the human hand, requiring more motor units. Large, spaced-out axons in the WMS nerves may be explained by the larger muscles they innervate, which are needed for fight-or-flight responses [35]. Due to limited access, we were only able to obtain one suprascapular nerve from a formalin-fixed human cadaver rather than a fresh specimen, so no statistics were run for the histological analysis of this nerve. The WMS suprascapular nerve originated from C5 and C6 (Fig. 2). The WMS suprascapular nerve was much larger and contained larger axons than the human suprascapular nerve (Fig. 6). These large suprascapular nerves with numerous large axons in the WMS are probably a function of their larger and stronger girdle muscles, possibly correlating with the swine's greater reliance on this region for mechanical support during movement.

The age discrepancy and underlying conditions of the fresh human cadavers are limitations of this study (Table 1). It is difficult to obtain fresh human samples that are uniform with regards to sex, weight, and age, and not complicated by differences in lifestyle, nutrition, occupation, etc. In this study, the swine were all male of similar age and weight whereas the humans varied in sex, age, and weight. Interestingly, despite these differences, the current observations were consistent across all three human subjects.

Table 1
Fresh Human Cadavers

Sex	*Age*	*Underlying Conditions*
Male	57	Hepatitis C
Female	61	Neuropathy
Male	34	None

In terms of modeling the average human, the conventional pig breed would be approximately 3-month-old. This creates problems because pigs do not reach sexual maturity until 6 months of age and are rapidly growing. Moreover, the conventional breeds are not pratical for long term studies, because the rapid rate of growth and remodeling would produce abnormal healing and poorly model nerve healing in human. The WMS attain an average human size at full maturity and maintain it for years.

Conclusions

Although there are differences between WMS brachial plexus and the human brachial plexus, they are close in size with similar composition and origin overall, making them a suitable animal model for BPI. In order to better determine if WMS would be an ideal model for researching BPI treatments, future studies should be conducted to investigate the pathological mechanisms and clinical effects of BPI in WMS.

Abbreviations

BPA: Brachial plexus avulsion

BPI: Brachial plexus injury

IACUC: Institutional Animal Care and Use Committee

SRTC: Swine Research and Teaching Center

WMS™: Wisconsin Miniature Swine™

Declarations

Ethics approval and consent to participate

All experiments involving animals were conducted under protocols approved by the University of Wisconsin-Madison Institutional Animal Care and Use Committee (IACUC) in accordance with published NIH and USDA guidelines.

Consent for publication

Not applicable

Availability of data and materials

The datasets during and/or analysed during the current study available from the corresponding author on reasonable request.

Competing interests

Dr. Shanmuganayagam is a co-inventor of the Wisconsin Miniature Swine™ for Biomedical Research, licensing of which as a biological material is assigned to the Wisconsin Alumni Research Foundation (WARF) [WARF: P130271US01].

Funding

Biomedical & Genomic Research Group Discretionary Fund (UW-Madison)

Neurofibromatosis Network, NF North Central and The NF Team

Authors' contributions

AH: Study concept and design, data acquisition including all animal dissections and human fixed cadaver dissection, data analysis and interpretation, drafting of the manuscript and critical revision

DH: Study concept and design, data acquisition, data analysis and interpretation, statistical analysis, drafting of the manuscript and critical revision

DTS: Study concept and design, data acquisition, drafting of the manuscript and critical revision

SMS: Human fresh tissue harvest, data analysis and interpretation

ML: Data acquisition, drafting of the manuscript and critical revision

LW: Data acquisition, drafting of the manuscript and critical revision

BH: Data acquisition, drafting of the manuscript and critical revision

BO: Data acquisition

DS (last): Study concept and design, data acquisition, drafting of the manuscript and critical revision

All authors read and approved the final manuscript.

Acknowledgements

The authors would like to acknowledge people who donate their bodies after death for teaching and/or research.

References

1. Midha R. Epidemiology of brachial plexus injuries in a multitrauma population. Neurosurgery. 1997;40:1182–8. discussion 1188–1189.
2. Moiyadi AV, Devi BI, Nair KP. Brachial plexus injuries: outcome following neurotization with intercostal nerve. J Neurosurg. 2007;107:308–13.
3. Gilbert WM, Nesbitt TS, Danielsen B. Associated factors in 1611 cases of brachial plexus injury. Obstet Gynecol. 1999;93:536–40.
4. Krishnan KG, Martin KD, Schackert G. Traumatic lesions of the brachial plexus: an analysis of outcomes in primary brachial plexus reconstruction and secondary functional arm reanimation. Neurosurgery. 2008;62:873–85. discussion 885 – 876.
5. Ali ZS, Johnson VE, Stewart W, Zager EL, Xiao R, Heuer GG, Weber MT, Mallela AN, Smith DH. Neuropathological Characteristics of Brachial Plexus Avulsion Injury With and Without Concomitant Spinal Cord Injury. J Neuropathol Exp Neurol. 2016;75:69–85.
6. Bruxelle J, Travers V, Thiebaut JB. **Occurrence and treatment of pain after brachial plexus injury**. *Clin Orthop Relat Res* 1988:87–95.
7. Vannier JL, Belkheyar Z, Oberlin C, Montravers P. [Management of neuropathic pain after brachial plexus injury in adult patients: a report of 60 cases]. Ann Fr Anesth Reanim. 2008;27:890–5.
8. Guo WL, Qi ZP, Yu L, Sun TW, Qu WR, Liu QQ, Zhu Z, Li R. Melatonin combined with chondroitin sulfate ABC promotes nerve regeneration after root-avulsion brachial plexus injury. Neural Regen Res. 2019;14:328–38.
9. Ham TR, Leipzig ND. Biomaterial strategies for limiting the impact of secondary events following spinal cord injury. Biomed Mater. 2018;13:024105.
10. Blits B, Carlstedt TP, Ruitenberg MJ, de Winter F, Hermens WT, Dijkhuizen PA, Claasens JW, Eggers R, van der Sluis R, Tenenbaum L, et al. Rescue and sprouting of motoneurons following ventral root avulsion and reimplantation combined with intraspinal adeno-associated viral vector-mediated expression of glial cell line-derived neurotrophic factor or brain-derived neurotrophic factor. Exp Neurol. 2004;189:303–16.
11. Yang J, Li X, Hou Y, Yang Y, Qin B, Fu G, Qi J, Zhu Q, Liu X, Gu L. Development of a novel experimental rat model for brachial plexus avulsion injury. Neuroreport. 2015;26:501–9.
12. Chuang DC. Brachial plexus injury: nerve reconstruction and functioning muscle transplantation. Semin Plast Surg. 2010;24:57–66.
13. Midha R. Nerve transfers for severe brachial plexus injuries: a review. Neurosurg Focus. 2004;16:E5.
14. Gao KM, Hu JJ, Lao J, Zhao X. Evaluation of nerve transfer options for treating total brachial plexus avulsion injury: A retrospective study of 73 participants. Neural Regen Res. 2018;13:470–6.
15. Zurita M, Aguayo C, Bonilla C, Otero L, Rico M, Rodriguez A, Vaquero J. The pig model of chronic paraplegia: a challenge for experimental studies in spinal cord injury. Prog Neurobiol. 2012;97:288–303.

16. Lee JH, Jones CF, Okon EB, Anderson L, Tigchelaar S, Kooner P, Godbey T, Chua B, Gray G, Hildebrandt R, et al. A novel porcine model of traumatic thoracic spinal cord injury. J Neurotrauma. 2013;30:142–59.
17. Dietz V, Curt A. Translating preclinical approaches into human application. Handb Clin Neurol. 2012;109:399–409.
18. Schomberg DT, Miranpuri GS, Chopra A, Patel K, Meudt JJ, Tellez A, Resnick DK, Shanmuganayagam D. **Translational Relevance of Swine Models of Spinal Cord Injury**. *J Neurotrauma* 2016.
19. Dolezalova D, Hruska-Plochan M, Bjarkam CR, Sorensen JC, Cunningham M, Weingarten D, Ciacci JD, Juhas S, Juhasova J, Motlik J, et al. Pig models of neurodegenerative disorders: Utilization in cell replacement-based preclinical safety and efficacy studies. J Comp Neurol. 2014;522:2784–801.
20. Hou X, Li C, Gu W, Guo Z, Yin W, Zhang D. Effect of Shenfu on inflammatory cytokine release and brain edema after prolonged cardiac arrest in the swine. Am J Emerg Med. 2013;31:1159–64.
21. Dawson HD, Loveland JE, Pascal G, Gilbert JG, Uenishi H, Mann KM, Sang Y, Zhang J, Carvalho-Silva D, Hunt T, et al. Structural and functional annotation of the porcine immunome. BMC Genom. 2013;14:332.
22. Tumbleson MEaS LB. Advances in Swine in Biomedical Research. New York: Plenum Press; 1996.
23. Wilson S, Fredericks DC, Safayi S, DeVries-Watson NA, Holland MT, Nagel SJ, Gillies GT, Howard MA. 3rd: **Ovine Hemisection Model of Spinal Cord Injury**. *J Invest Surg* 2019:1–13.
24. Wilson S, Abode-Iyamah KO, Miller JW, Reddy CG, Safayi S, Fredericks DC, Jeffery ND, DeVries-Watson NA, Shivapour SK, Viljoen S, et al. An ovine model of spinal cord injury. J Spinal Cord Med. 2017;40:346–60.
25. Stern S, Rice J, Philbin N, McGwin G, Arnaud F, Johnson T, Flournoy WS, Ahlers S, Pearce LB, McCarron R, Freilich D. Resuscitation with the hemoglobin-based oxygen carrier, HBOC-201, in a swine model of severe uncontrolled hemorrhage and traumatic brain injury. Shock. 2009;31:64–79.
26. Torres-Rovira L, Astiz S, Caro A, Lopez-Bote C, Ovilo C, Pallares P, Perez-Solana ML, Sanchez-Sanchez R, Gonzalez-Bulnes A. Diet-induced swine model with obesity/leptin resistance for the study of metabolic syndrome and type 2 diabetes. ScientificWorldJournal. 2012;2012:510149.
27. Fox CH, Johnson FB, Whiting J, Roller PP. Formaldehyde fixation. J Histochem Cytochem. 1985;33:845–53.
28. Di Scipio F, Raimondo S, Tos P, Geuna S. A simple protocol for paraffin-embedded myelin sheath staining with osmium tetroxide for light microscope observation. Microsc Res Tech. 2008;71:497–502.
29. Hanna A. The SPA arrangement of the branches of the upper trunk of the brachial plexus: a correction of a longstanding misconception and a new diagram of the brachial plexus. J Neurosurg. 2016;125:350–4.
30. Penas C, Casas C, Robert I, Fores J, Navarro X. Cytoskeletal and activity-related changes in spinal motoneurons after root avulsion. J Neurotrauma. 2009;26:763–79.

31. Koliatsos VE, Price WL, Pardo CA, Price DL. Ventral root avulsion: an experimental model of death of adult motor neurons. J Comp Neurol. 1994;342:35–44.
32. Miranpuri GS, Schomberg DT, Stan P, Chopra A, Buttar S, Wood A, Radzin A, Meudt JJ, Resnick DK, Shanmuganayagam D. Comparative Morphometry of the Wisconsin Miniature Swine(TM) Thoracic Spine for Modeling Human Spine in Translational Spinal Cord Injury Research. Ann Neurosci. 2018;25:210–8.
33. Septimus Sisson JDG, Robert Getty **Spinal nerves**: **pig**. In *Sisson and Grossman's the Anatomy of the Domestic Animals. Volume* 5. Edited by Guanabara Koogan. Rio de Janeiro: W B Saunders Co; 1986: 1294–1319.
34. Santos Lea. ORIGIN AND DISTRIBUTION OF THE BRACHIAL PLEXUS IN WILD BOAR. Journal of Bioscience. 2015;31:1816–25.
35. Lavelle MJSN, Ellis CK, Halseth JM, Glow MP, VanNatta EH, Sanders HN, VerCauteren KC. When pigs fly: Reducing injury and flight response when capturing wild pigs. Appl Anim Behav Sci. 2019;215:21–5.

Figures

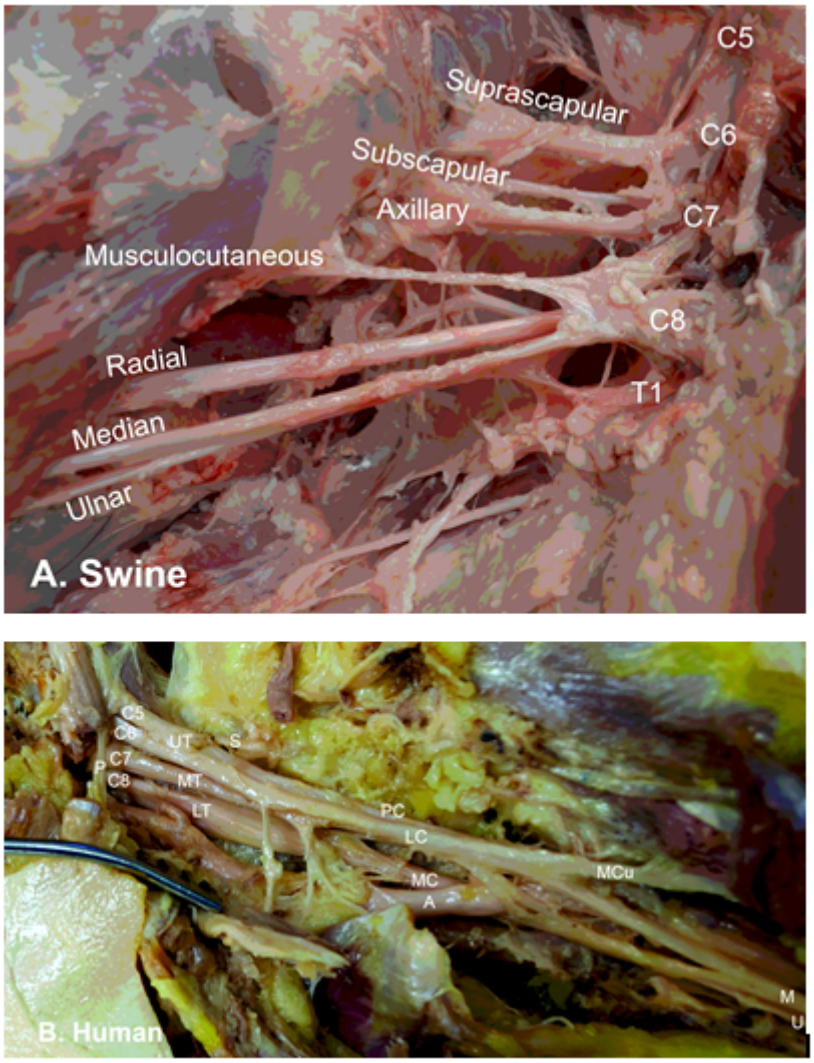

Figure 1

A. Anterior exposure of the swine right brachial plexus. The swine model lacks the presence of a clavicle. The separation into 3 trunks and 3 cords is significantly less developed in the swine. There is rather upper (C6), middle (C7), and lower (C8) systems with ventral and dorsal components. B. Left human brachial plexus, anterior view, the clavicle has been removed. UT = upper trunk, MT = middle trunk, LT = lower trunk, S = suprascapular, PC = posterior cord, LC = lateral cord, MC = medial cord, MCu = musculocutaneous, M = median, U = ulnar, A = axillary artery.

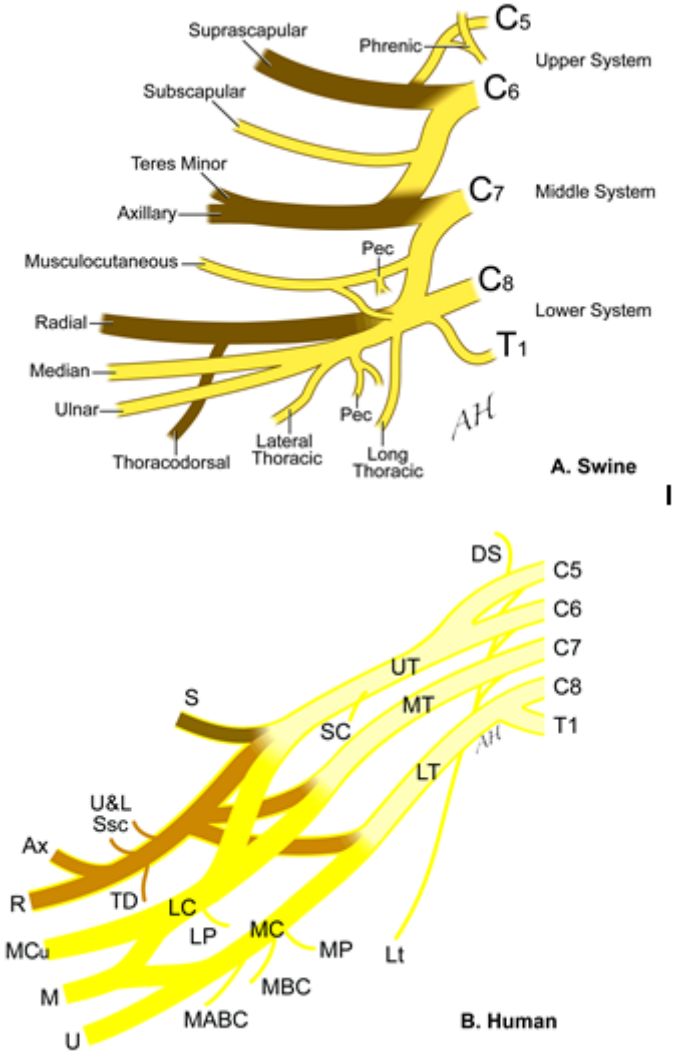

Figure 2

A. Diagrammatic representation of the swine brachial plexus. Pec = pectoral. Copyright AH. Published with permission. B. Diagram of the human brachial plexus. DS = dorsal scapular, Lt = long thoracic, UT = upper trunk, MT = middle trunk, LT = lower trunk, SC = subclavius, S = suprascapular, PC = posterior cord, LC = lateral cord, MC = medial cord, U&L Ssc = upper and lower subscapular, TD = thoracodorsal, Ax: axillary, R = radial, LP = lateral pectoral, MCu = musculocutaneous, M = median, U = ulnar, MP = medial pectoral, MBC = medial brachial cutaneous, MABC = medial antebrachial cutaneous. Reproduced from. Hanna: The SPA arrangement of the branches of the upper trunk of the brachial plexus: a correction of a long-standing misconception and a new diagram of the brachial plexus. J Neurosurg 125:350-354, 2016. Copyright Amgad Hanna. Published with permission. Note that the arrangement into trunks and cords is not as obvious in the swine, there are rather upper, middle, and lower systems.

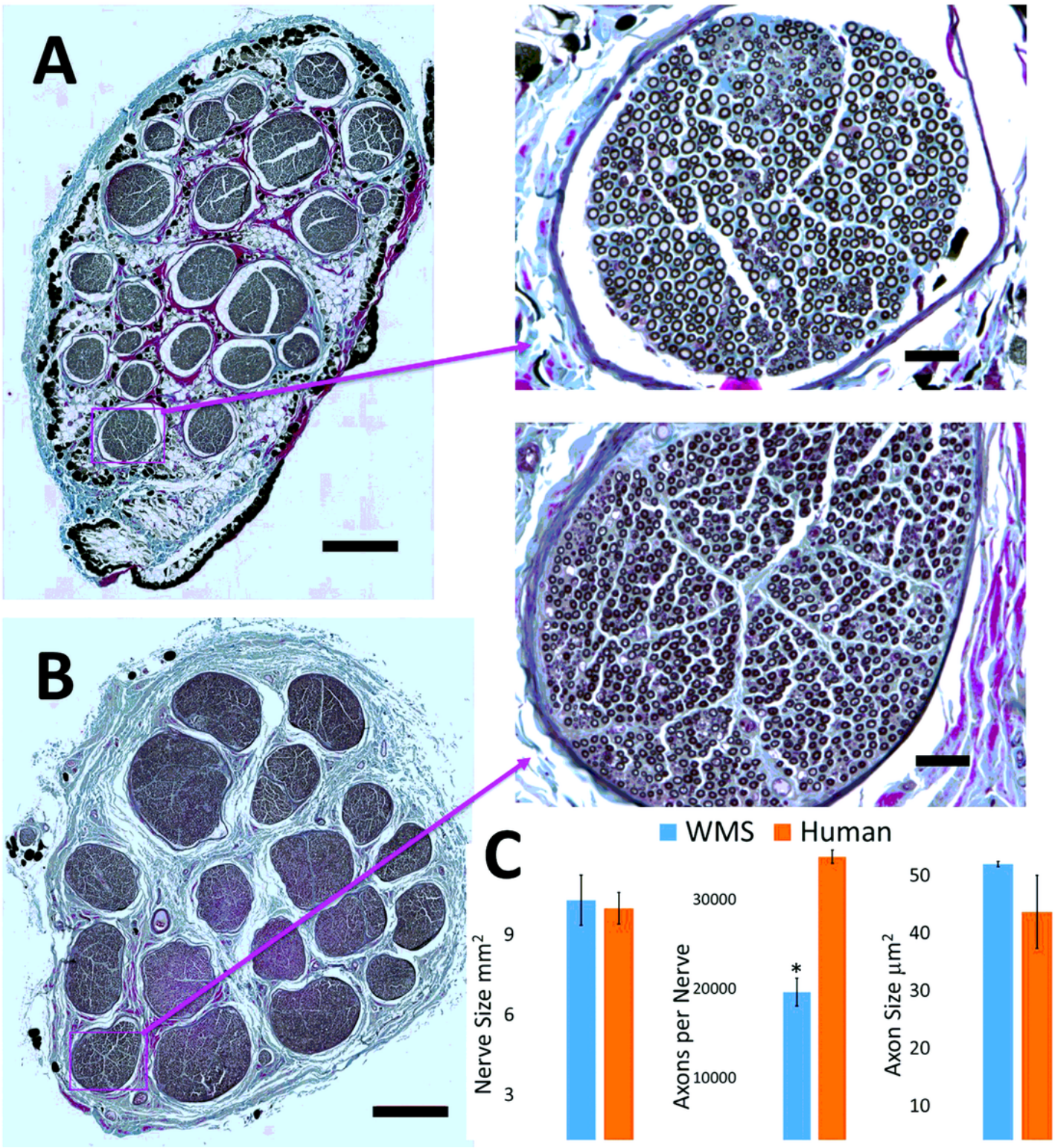

Figure 3

Histological analyses of the median nerve. Myelinated axons were analyzed on transverse sections of WMS median nerve (A) and compared to transverse sections of human median nerve (B). Although there were significantly fewer myelinated axons in the WMS median nerve, the cross-sectional area of the WMS median nerve was not significantly different from human nerves, and the axon size was not significantly

different (C). Scale bars: 500 μm on whole nerve images and 50 μm on higher magnification images; *p < 0.05 (Student's T-Test); error bars represent ± SEM; n = 3.

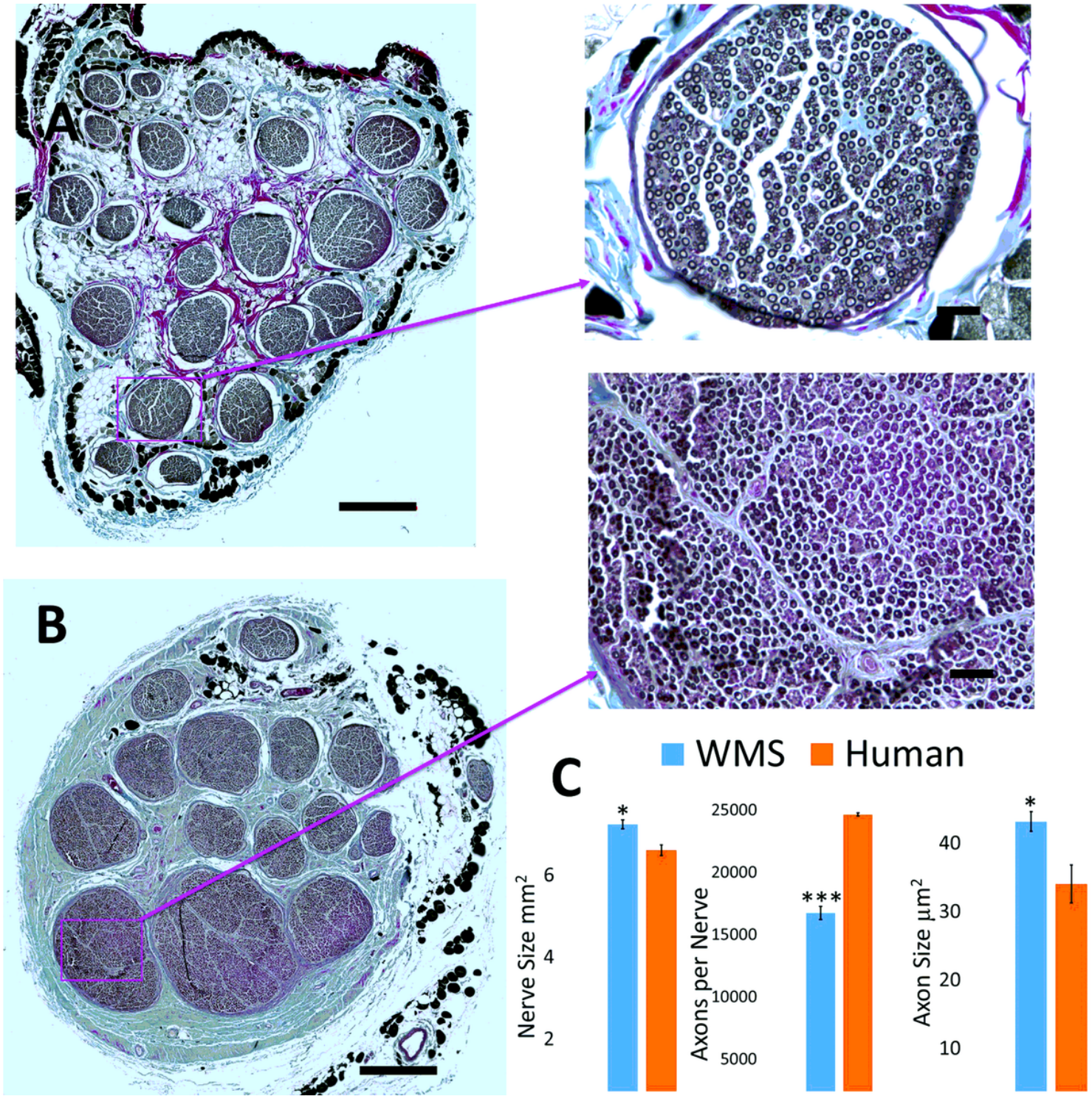

Figure 4

Histological analyses of the ulnar nerve. Myelinated axons were analyzed on transverse sections of WMS ulnar nerve (A) and compared to transverse sections of human ulnar nerve (B). The cross-sectional area of the WMS ulnar nerve was significantly larger than human ulnar nerves. Although there were significantly fewer myelinated axons in the WMS ulnar nerve, the axons in WMS ulnar nerves were

significantly larger than in human ulnar nerves (C). Scale bars: 500 µm on whole nerve images and 50 µm on higher magnification images; *p < 0.05,***p < 0.001 (Student's T-Test); error bars represent ± SEM; n = 3.

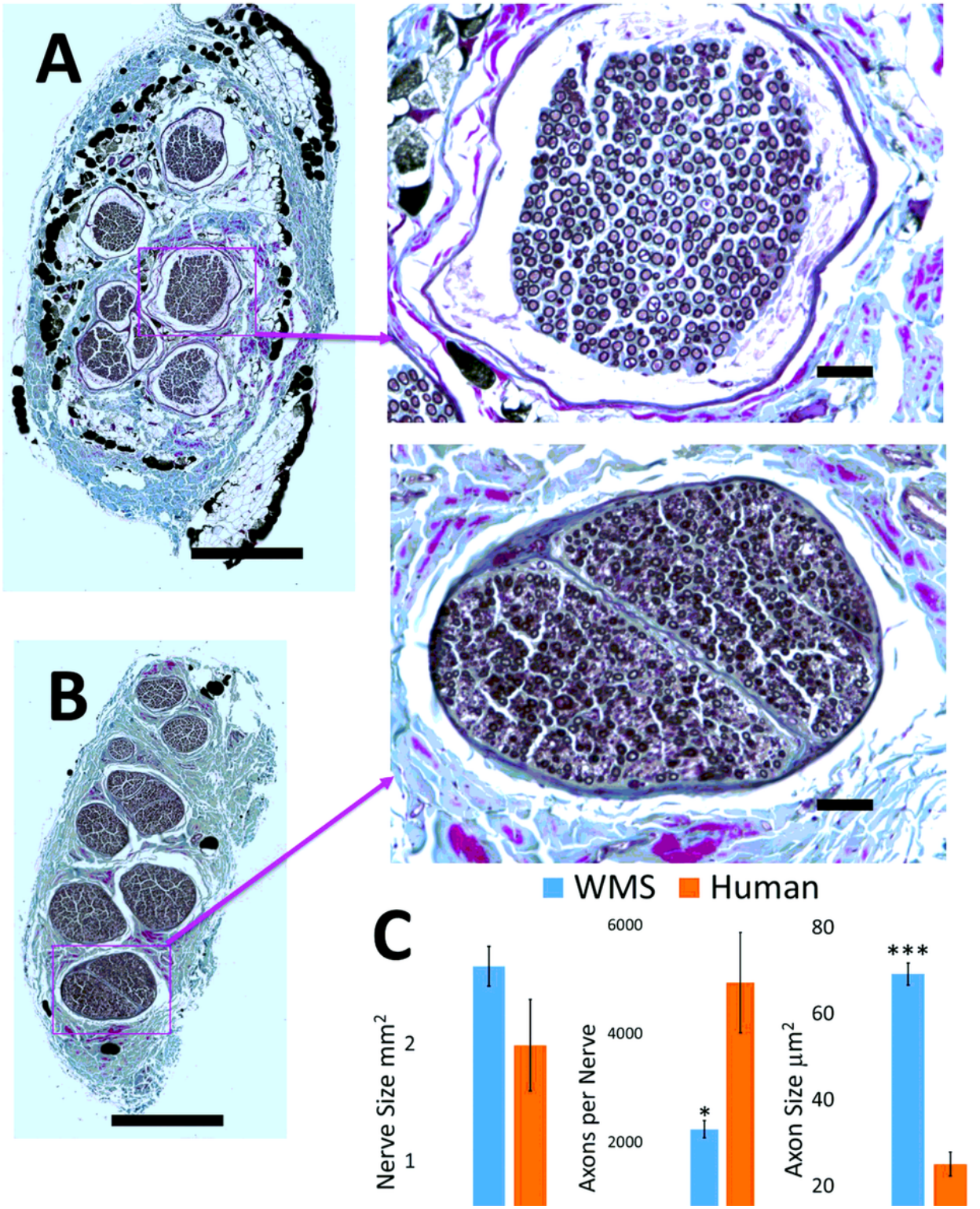

Figure 5

Histological analyses of the musculocutaneous nerve. Myelinated axons were analyzed on transverse sections of WMS musculocutaneous nerve (A) and compared to transverse sections of human

musculocutaneous nerve (B). The cross-sectional area of the WMS musculocutaneous nerve was not significantly different than human musculocutaneous nerves. Although there were significantly fewer myelinated axons in the WMS musculocutaneous nerve, the axons in WMS musculocutaneous nerves were significantly larger than in human musculocutaneous nerves (C). Scale bars: 500 μm on whole nerve images and 50 μm on higher magnification images; *p < 0.05,***p < 0.001 (Student's T-Test); error bars represent ± SEM; n = 3.

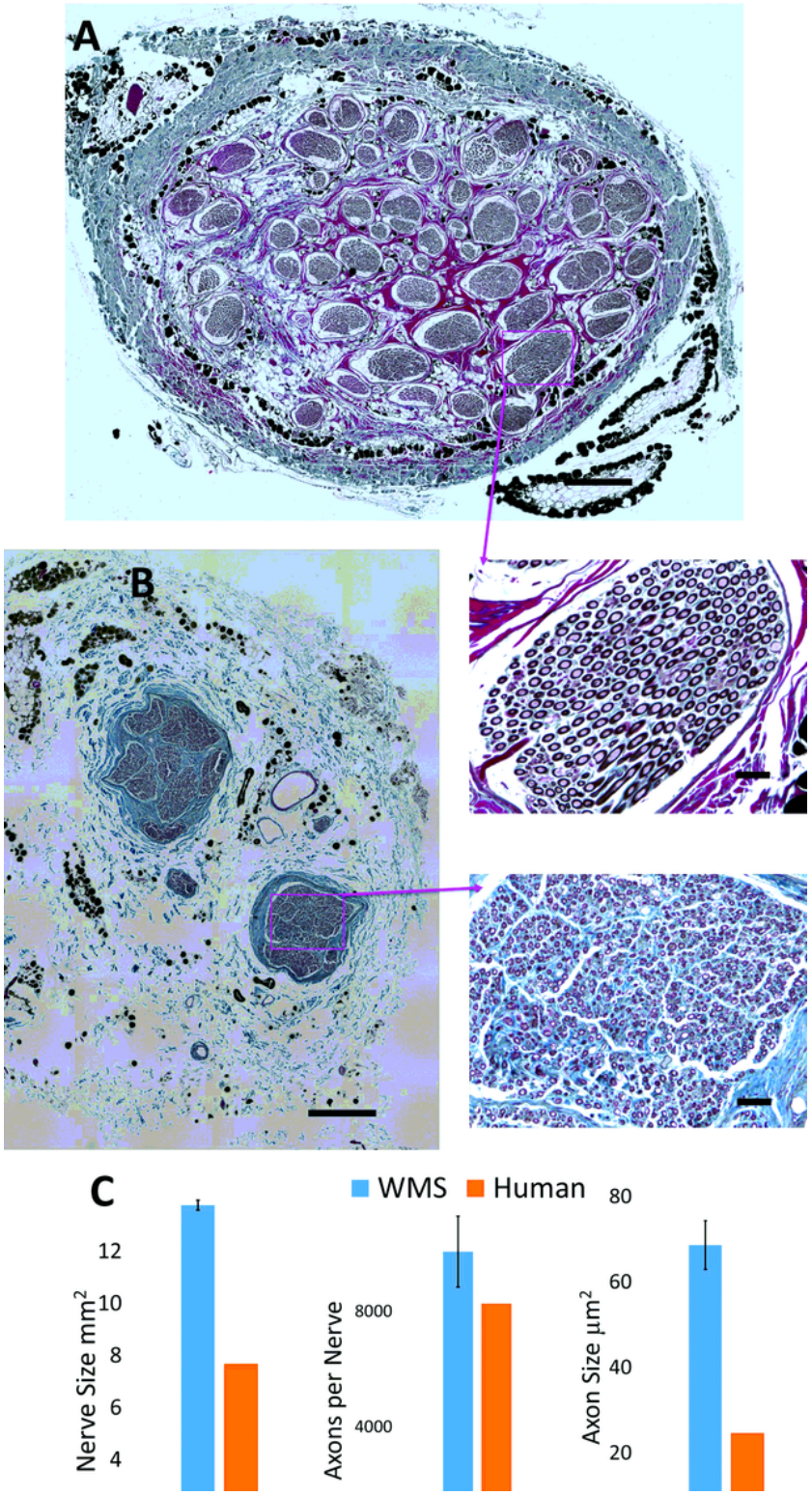

Figure 6

Histological analyses of the suprascapular nerve. Myelinated axons were analyzed on a transverse section of WMS suprascapular nerve (A) and compared to transverse sections of human suprascapular nerve (B). The total nerve cross-sectional area, number of myelinated axons and size of axons were quantified (C). Scale bars: 500 μm on whole nerve images and 50 μm on higher magnification images; error bars represent ± SEM; WMS n = 3, human cadaver n = 1.